# Adsorption of Equal Mass Fraction Near an Azeotropic Mixture of Pentafluoroethane and 1,1,1-Trifluoroethane on Activated Carbon

**Bidyut B. Saha, Ibrahim I. El-Sharkawy,[†] Khairul Habib, Shigeru Koyama, and Kandadai Srinivasan***

Interdisciplinary Graduate School of Engineering Sciences, Kyushu University, Kasuga-koen 6-1, Kasuga-shi, Fukuoka 816-8580, Japan

This paper presents adsorption isotherms for R-507A, which is a near azeotropic mixture of R-125 (pentafluoroethane) and R-143a (1,1,1-trifluoroethane) in equal mass fractions, on a Maxsorb III specimen of activated carbon in the temperature range of about (5 to 70) °C and pressure up to 15 bar. The data were obtained using the desorption method to an estimated precision of 5 % and fitted to three isotherm equations, namely, Dubinin−Astakhov, Langmuir, and Tóth. The adsorption parameters were determined. Some peculiarities in isosteric heating behavior were observed.

## Introduction

Refrigerant 507A, which is a near azeotropic mixture of equal mass fractions of pentafluoroethane (R-125) and 1,1,1-trifluoroethane (R-143a), is used as a refrigerant for low- and medium-temperature supermarket refrigeration and is also used for cascading with carbon dioxide refrigeration for low-temperature freezers.[1] Concerns of global warming due to refrigeration systems arise because of two factors. The first is the direct emission of refrigerant, which has a warming impact of more than 3000 relative to carbon dioxide. Refrigerant leakage can be as high as 10 % of charge per year.[2] The second is the greenhouse gas emission arising due to compression work. Measurement of adsorption isotherms for R-507A on a highly microporous activated carbon such as Maxsorb III is motivated by three exigencies. The first one is the need to capture this refrigerant's emissions using the adsorption route. The second is the urge to supplement energy needs of a mechanical compressor with solid sorption based thermal compression in a stand-alone or hybrid mode. The third is to generate data that could be used in adsorption theories since there have been very few experimental measurements on azeotropic refrigerant mixtures.

Consequent to confirmation of stratospheric ozone depletion accelerated by chlorofluorocarbon refrigerants, capturing refrigeration emissions has also been the prime driver for numerous adsorption measurements on various adsorbents (such as activated carbons, zeolites, and silica gel) for this class of refrigerants. As a result, a majority of them focus on adsorption at subatmospheric or near atmospheric pressures. A review of work on the recovery of the ethane and propane family HCFC recovery is provided by Tsai.[3] Adsorption data for other ASHRAE designated refrigerants 11, 12, 13, 14, 22, 113, 115, 116, 123, 134a, 141b, and 318 are available in the literature.[4–17] There are some above atmospheric pressure studies for adsorption of R-12, R-22, and R-115 at pressures to 602 kPa[6] and for HFC 134a and pressures up to 1.3 MPa.[14,15]

* Corresponding author. Fax: +61 3 9584 5624. E-mail: mecks@hotmail.com. Currently at Frigrite Refrigeration Pty. Ltd., 27 Grange Road, Cheltenham Vic 3192, Australia.
[†] Permanent address: Mechanical Power Engineering Department, Faculty of Engineering, Mansoura University, El-Mansoura, Egypt.

The data of Akkimaradi et al.[14] were utilized by Akkimaradi et al.[18] and Banker et al.[19] for an analysis and to build a refrigeration system with Maxsorb II as the adsorbent and HFC 134a as the refrigerant.[20] Adsorption data play an important role in sizing of the thermal compression hardware and for determining the heat inventories for operation of the cycle. Saha et al.[21] have shown that the adsorption refrigeration systems can be powered by heat sources at as low as 50 °C. The objective of this paper is to report data for adsorption of R-507A on Maxsorb III in the pressure and temperature range of interest for development of thermal compression systems. The method used is the desorption method first proposed by Prakash et al.[22] for nitrogen adsorption and further improved by Saha et al.[23] for methane adsorption on Maxsorb III.

## Materials and Methods

***Activated Carbon and the R-507A.*** The Maxsorb specimen labeled MSC-30 was supplied by the Kansai Coke and Chemicals Company (Batch No. 03-07061) with a stated surface area of 3140 $m^2 \cdot g^{-1}$ and a micropore volume ($v_\mu$) of 1.7 $cm^3 \cdot g^{-1}$. It has a mean particle diameter of 72 $\mu$m, an ash content of no more than 0.1 %, and moisture of no more than 0.8 %. Its pH is 4.1. The pore size distribution obtained through nonlocal density functional theory (NLDFT) shows a peak at 2 nm confirming the highly microporous nature of the specimen used.[23] The sample of R-507A used is 99.999 % pure and was supplied by the Asahi Glass Co., Japan.

***Experimental Apparatus.*** The experimental apparatus is shown in Figure 1, and measurement procedures were described in detail elsewhere; hence only a brief outline will be given herein.[23] The adsorption cell is a slender cylindrical unit of internal dimensions of 30 mm diameter and 300 mm depth giving an enclosed volume ($V_{cell}$) of ~212 cc. It has been designed to withstand pressures to 50 bar even at 150 °C. It was packed with 65.66 g of the activated carbon ($m_{ch}$) specimen mentioned above, giving a net packing density of 0.31 $g \cdot cm^{-3}$. The external plumbing is made up of 1/4" nominal stainless steel tubes with an internal diameter of 4.35 mm and a set of Swagelok fittings (valves, T's, and crosses). The total internal plumbline volume is estimated to be 13.1 $cm^3$. A filter of 2 $\mu$m stainless steel fine mesh that is capable of stopping migration

10.1021/je800204p CCC: $40.75 © 2008 American Chemical Society
Published on Web 07/19/2008

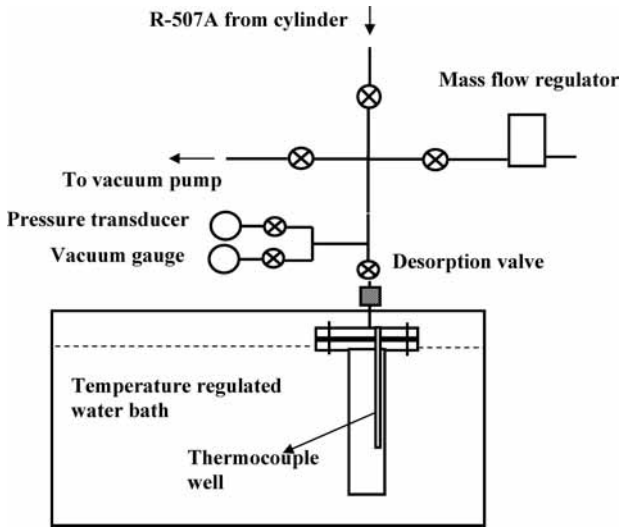


**Figure 1.** Schematic arrangement of the desorption apparatus.

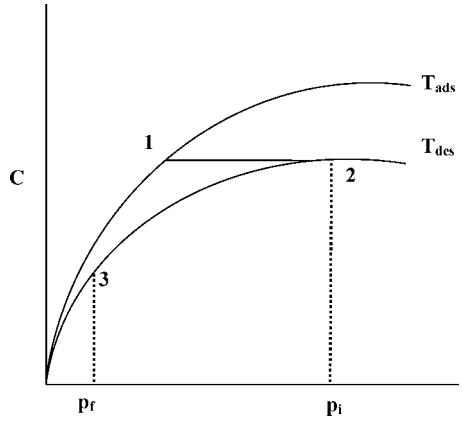


**Figure 2.** Sequence of charging, heating, and desorption.

of activated carbon particles during evacuation and desorption was fitted in the plumbline at the exit of the cell.

***Instrumentation.*** The instrumentation consists of (i) a 10 standard liters per minute (at 20 °C and 1.013 bar) mass flow regulator (Kojima-Kofloc-5100) that has a measurement uncertainty of ± 1 % of full scale (1.67 $cm^3 \cdot s^{-1}$), (ii) a Kyowa-PGS-50KA 50 bar pressure transducer with an uncertainty in measurement of ± 0.1 % of full scale, (iii) a series of type K thermocouples (supplied by Chino Corp., Japan, uncertainty of ± 0.6 °C traceable to Japan Calibration Service System standards) precalibrated against a platinum resistance thermometer in a precision temperature bath for measuring temperatures of the adsorbent in the cell, the thermostatic bath in which the entire cell is immersed, and the ambient, and (iv) a Keithtly 2700 data acquisition system connected to a computer. Data were logged at about 1 s intervals over the entire duration of each process, namely, adsorption, isosteric heating, desorption, and isosteric cooling. The circulating water bath could give a stability of ± 0.1 °C.

***Experimental Procedures.*** The adsorption cell was subjected to repeated filling, baking, and evacuation sequences to ensure that any residual gas is only R-507A. The sequence of operations is depicted in Figure 2. The cell is filled slowly with R-507A with the cell at a temperature between (5 and 30) °C ($T_{ads}$). To ensure that there is no condensation of R-507A in the lines nor in the cell, the filling pressure ($p_1$) is always less than the saturation pressure ($p_{sdes}$) corresponding to the desorption temperature of the cell and that corresponding to the ambient ($p_{sa}$). After the cell has stabilized (at state 1 in Figure 2), it is isolated and then slowly heated (over several hours) to the desired temperature of the isotherm (state 2 in Figure 2). When the cell reaches equilibrium at the set point of the isotherm, its pressure at that state is taken as the pressure on the isotherm before desorption ($p_i$). The cell is gradually desorbed over periods of the order of several 100's of seconds until the flow rate falls to a value that is one order of magnitude higher than the uncertainty of the mass flow regulator. The pressure of the cell is allowed to stabilize (at state 3 in Figure 2), which gives the final pressure after desorption on the isotherm ($p_f$).

The primary data are the time-dependent flow rate through the mass flow regulator, the initial and final cell pressures ($p_i$ and $p_f$), and cell and ambient temperatures ($T_{cell}$ and $T_a$). The flow data are directly reduced to standard liters desorbed (Std $L_{des}$) by numerical integration of the flow record and converted to total mass desorbed using standard conditions specified by the flow meter manufacturer. This desorbed mass needs to be corrected for the internal cell void and the pipeline volume.[23] The void volume ($V_{void}$) is calculated as follows

$$V_{void} = V_{cell} - \frac{m_{ch}}{\rho_s} - v_\mu m_{ch} \tag{1}$$

Since 65.66 g of carbon has been packed into the cell of 211.95 $cm^3$, assuming a solid carbon density ($\rho_s$) of 2.2 $g \cdot cm^{-3}$, the cell void is 70.5 $cm^3$. The desorbed mass corrections are defined as follows

$$\Delta m_{void} = V_{void}[\rho_i(p_i, T_{des}) - \rho_f(p_f, T_{des})] \tag{2}$$

$$\Delta m_{pipe} = V_{pipe}[\rho_i(p_i, (T_{des} + T_a)/2) - \rho_f(p_f, (T_{des} + T_a)/2)] \tag{3}$$

where $\rho$ is the density of R-507A and subscripts i and f refer to initial final states. Since the plumbline volume is only about 6 % of the cell volume, its effect is rather marginal. The density data for R-507A are calculated using the program REFPROP.[24] Table 1 gives the raw data.

## Correlation of data

The isotherm equations to which the data are regressed to are the Langmuir, Tóth, and Dubinin−Astakhov (DA) equations in the following form

$$\frac{C}{C_o} = \frac{k_0 e^{\frac{\Delta h_{st}}{RT}} p}{1 + k_0 e^{\frac{\Delta h_{st}}{RT}} p} \tag{4}$$

$$\frac{C}{C_o} = \frac{k_0 e^{\frac{\Delta h_{st}}{RT}} p}{\left[1 + \left(k_0 e^{\frac{\Delta h_{st}}{RT}} p\right)^t\right]^{1/t}} \tag{5}$$

$$W = W_o e^{-\left[\frac{RT}{E} \ln\left(\frac{p_s}{p}\right)\right]^n} \tag{6}$$

where $C$ is the mass concentration ($g \cdot g^{-1}$); $W = Cv_a$; $v_a$ is the adsorbed phase specific volume; and $R$ is the universal gas constant (8.314 $J \cdot mol^{-1} \cdot K^{-1}$). In the case of DA eq 6, the adsorbed phase volume is calculated as[14]

$$v_a = v_b \exp[\Omega(T_{des} - T_b)] \tag{7}$$

where

$$\Omega = \frac{\ln\left(\frac{b}{v_b}\right)}{(T_c - T_b)} \tag{8}$$

In the above equation, subscripts b and c refer to normal boiling and critical points. For R-507A, $T_c$ = 343.8 K, $T_b$ = 226.4 K,

**Table 1. Raw Adsorption Data for R-507A from All Experiments**

| $T_{des}$/°C | $T_a$/°C | $p_i$/bar | $p_f$/bar | Std $L_{des}$ | $\Delta m_{void}$/g | $\Delta m_{pipe}$/g | $\Delta C$/g·g$^{-1}$ |
|---|---|---|---|---|---|---|---|
| 4.6 | 15.9 | 6.35 | 2.43 | 6.16 | 1.48 | 0.26 | 0.337 |
| 18.9 | 16.5 | 10.31 | 2.63 | 9.17 | 2.96 | 0.56 | 0.488 |
| 19.1 | 28.8 | 9.60 | 1.99 | 11.48 | 2.82 | 0.51 | 0.627 |
| 19.2 | 20.3 | 4.44 | 1.78 | 6.80 | 0.86 | 0.16 | 0.386 |
| 24.1 | 27.7 | 10.79 | 2.06 | 11.94 | 3.23 | 0.59 | 0.647 |
| 24.2 | 20.5 | 5.16 | 1.89 | 7.26 | 1.05 | 0.20 | 0.409 |
| 24.2 | 25.1 | 6.91 | 1.89 | 9.74 | 1.67 | 0.31 | 0.545 |
| 29.0 | 29.2 | 6.24 | 1.92 | 8.75 | 1.38 | 0.26 | 0.492 |
| 29.1 | 28.1 | 4.24 | 1.91 | 5.62 | 0.71 | 0.13 | 0.319 |
| 29.1 | 30.1 | 10.56 | 2.07 | 11.87 | 3.01 | 0.56 | 0.646 |
| 29.1 | 28.9 | 7.81 | 2.08 | 10.02 | 1.90 | 0.35 | 0.557 |
| 29.2 | 28.9 | 9.42 | 2.26 | 10.72 | 2.47 | 0.46 | 0.588 |
| 29.2 | 28.4 | 12.20 | 1.99 | 12.83 | 3.78 | 0.71 | 0.689 |
| 29.2 | 27.7 | 3.45 | 1.91 | 3.99 | 0.47 | 0.09 | 0.227 |
| 29.3 | 20.6 | 5.83 | 2.02 | 7.44 | 1.21 | 0.23 | 0.417 |
| 29.4 | 24.5 | 7.83 | 2.08 | 9.74 | 1.90 | 0.36 | 0.540 |
| 33.9 | 13.5 | 9.90 | 2.62 | 9.81 | 2.48 | 0.50 | 0.534 |
| 34.3 | 19.6 | 6.58 | 2.08 | 8.08 | 1.41 | 0.27 | 0.451 |
| 34.4 | 24.1 | 9.35 | 1.89 | 11.32 | 2.47 | 0.48 | 0.624 |
| 39.1 | 32.2 | 6.84 | 2.07 | 8.48 | 1.47 | 0.28 | 0.474 |
| 39.2 | 29.8 | 8.60 | 2.00 | 10.42 | 2.10 | 0.40 | 0.577 |
| 39.2 | 31.5 | 8.10 | 2.01 | 9.90 | 1.92 | 0.36 | 0.550 |
| 39.2 | 21.7 | 7.94 | 2.17 | 8.86 | 1.81 | 0.35 | 0.490 |
| 39.3 | 30.7 | 7.20 | 2.26 | 8.10 | 1.53 | 0.29 | 0.450 |
| 39.3 | 31.2 | 5.96 | 2.10 | 7.18 | 1.17 | 0.22 | 0.403 |
| 39.3 | 30.7 | 4.68 | 1.99 | 5.69 | 0.80 | 0.15 | 0.322 |
| 39.3 | 31.8 | 10.68 | 2.02 | 12.31 | 2.87 | 0.55 | 0.674 |
| 39.3 | 30.5 | 5.53 | 2.29 | 6.00 | 0.98 | 0.19 | 0.336 |
| 39.3 | 30.1 | 9.68 | 1.95 | 11.61 | 2.50 | 0.48 | 0.640 |
| 39.3 | 26.2 | 10.26 | 2.46 | 10.22 | 2.58 | 0.50 | 0.556 |
| 44.1 | 23.5 | 8.85 | 1.82 | 10.67 | 2.18 | 0.43 | 0.590 |
| 54.2 | 22.5 | 11.47 | 1.93 | 11.75 | 2.93 | 0.60 | 0.640 |
| 59.1 | 22.3 | 12.74 | 1.82 | 12.88 | 3.34 | 0.70 | 0.699 |
| 63.9 | 20.1 | 15.12 | 3.48 | 12.18 | 3.68 | 0.81 | 0.651 |
| 69.0 | 18.2 | 11.60 | 2.46 | 10.00 | 2.63 | 0.56 | 0.542 |

and $v_b = 7.59 \cdot 10^{-4}$ m$^3$·kg$^{-1}$.[24] The Van der Waals volume $b = RT_c/8p_c$. Here, $p_c = 37.05$ bar,[24] yielding $b = 7.59 \cdot 10^{-4}$ m$^3$·kg$^{-1}$ and $\Omega = 2.14 \cdot 10^{-3}$ K$^{-1}$. The saturation vapor pressure is calculated using the Wagner equation.[25]

Since the difference in equilibrium concentrations between two pressures $p_i$ and $p_f$ along an isotherm $T_{des}$ is measured, the isotherm equations can be used to describe the desorption as follows

$$\Delta C_{T_{des}} = C_o \left[ \frac{k_0 e^{\frac{\Delta h_{st}}{RT_{des}}} p_i}{1 + k_0 e^{\frac{\Delta h_{st}}{RT_{des}}} p_i} - \frac{k_0 e^{\frac{\Delta h_{st}}{RT_{des}}} p_f}{1 + k_0 e^{\frac{\Delta h_{st}}{RT_{des}}} p_f} \right] \quad (9)$$

$$\Delta C_{T_{des}} = C_0 k_0 \left\{ \frac{e^{\frac{\Delta h_{st}}{RT_{des}}} p_i}{\left[1 + \left(k_0 e^{\frac{\Delta h_{st}}{RT_{des}}} p_i\right)^t\right]^{1/t}} - \frac{e^{\frac{\Delta h_{st}}{RT_{des}}} p_f}{\left[1 + \left(k_0 e^{\frac{\Delta h_{st}}{RT_{des}}} p_f\right)^t\right]^{1/t}} \right\} \quad (10)$$

$$\Delta C_{T_{des}} = W_o \frac{e^{-\left[\frac{RT_{des}}{E} \ln\left(\frac{p_s}{p_i}\right)\right]^n} - e^{-\left[\frac{RT_{des}}{E} \ln\left(\frac{p_s}{p_f}\right)\right]^n}}{v_a} \quad (11)$$

A regression analysis is made to secure the least-squares for deviations between experimental differential concentrations against the right-hand side of each of eqs 9 to 11. The entire calculation scheme has been programmed on a spreadsheet.

***Assessment of Overall Uncertainty.*** In addition to uncertainties associated with the instrumentation, averaging the cell temperature during desorption, and the void correction, there will be certain errors introduced due to mathematical regression resulting in deviations between the measured desorption and that obtained from the respective equations. It is expected that the overall uncertainty will be within ± 5 % with a minimum of 0.012 g·g$^{-1}$.

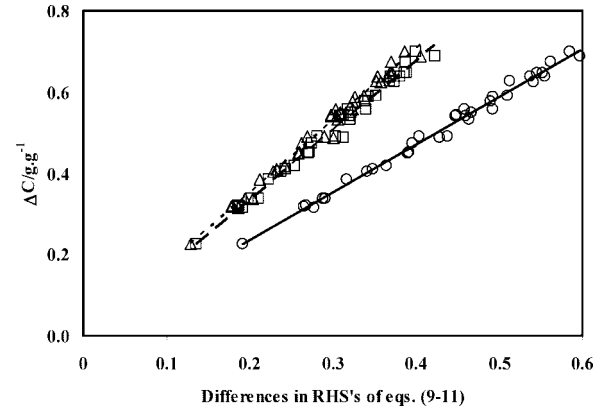


**Figure 3.** Differences in RHS's of eqs 9 to 11 vs $\Delta C$. □, Langmuir; Δ, Tóth; ○, DA.

**Table 2. Adsorption Parameters for Langmuir, Tóth, and DA Equations**

| parameter | Langmuir | Tóth | DA |
|---|---|---|---|
| $k_0$ | $1.93 \cdot 10^{-5}$ | $2.10 \cdot 10^{-5}$ | |
| $\Delta h_{st}$/J·mol$^{-1}$ | 23490 | 23460 | |
| $E$/J·mol$^{-1}$ | | | 5740 |
| $t$ or $n$ | | 0.93 | 1.47 |
| $C_0$/g·g$^{-1}$ | 1.702 | 1.778 | |
| $W_0$/cm$^3$·g$^{-1}$ | | | 1.175 |
| Ω | | | $2.138 \cdot 10^{-3}$ |
| average regression error/% | 3 | 3.1 | 2.3 |
| intercept | $-5.00 \cdot 10^{-3}$ | $-4.78 \cdot 10^{-3}$ | $1.07 \cdot 10^{-4}$ |

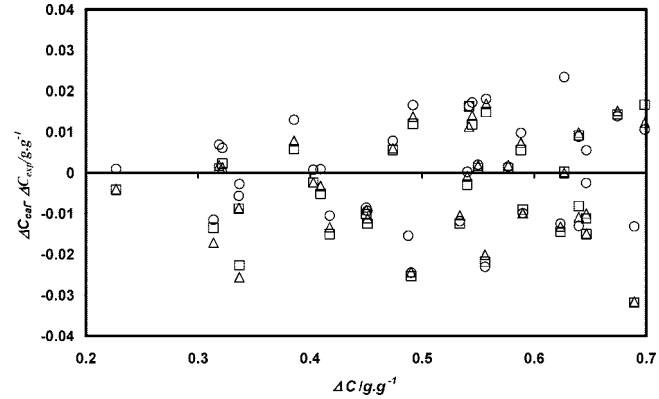


**Figure 4.** Comparison of deviations between calculated and experimental uptake differences. □, Langmuir; Δ, Tóth; ○, DA.

## Results and Discussion

Figure 3 shows a plot of differences on the right-hand sides of eqs 9 to 11 against measured $\Delta C$ for the condition of least-squares. The optimized values are $k_0$, $\Delta h_{st}$, $t$, $W_o$, $E$, and $n$ and are listed in Table 2. The intercept indicates the goodness of fit, which should be zero for a perfect fit.

Figure 4 makes a comparison of goodness of fits of all the isotherm equations wherein the deviations between experimental and calculated differences between fits are compared. As can be seen from data in Table 2, the DA equation gives a good description of the present measurements of R-507A adsorption on Maxsorb III. There is only a marginal improvement with the Tóth equation over the Langmuir equation.

There are some marginal differences, albeit within the limits of experimental uncertainties, between the three equations of

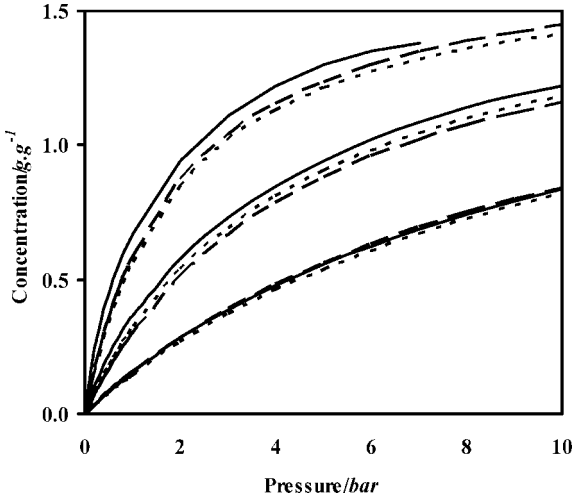


**Figure 5.** Comparison of all isotherm equations for isotherms at 5 (top) °C, 30 (middle) °C, and 60 (bottom) °C. ----, Langmuir; − − −, Tóth; —, DA.

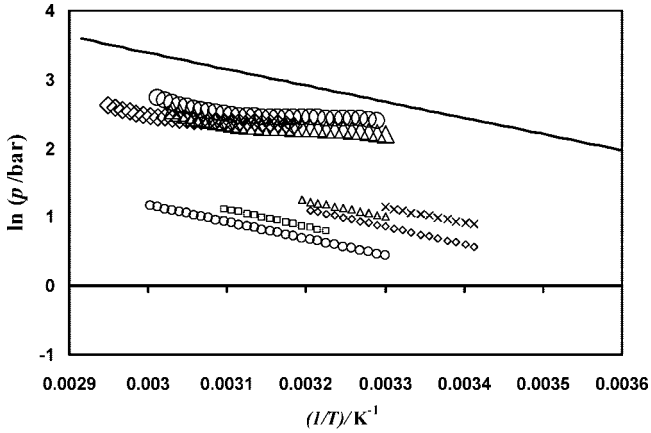


**Figure 6.** Pressure and temperature variations during isosteric heating/cooling. Small symbols: ○, $C/C_0 = 0.38$; □, $C/C_0 = 0.40$; ◇, $C/C_0 = 0.50$; Δ, $C/C_0 = 0.53$; ×, $C/C_0 = 0.59$. Large symbols: ◇, $C/C_0 = 0.79$; ○, $C/C_0 = 0.84$; Δ, $C/C_0 = 0.90$; full line, vapor pressure curve of pure R-507A.

isotherms considered here. A comparison of isotherms at a few temperatures is depicted in Figure 5.

It is possible to extract the isosteric heat of adsorption from pressure and temperature recordings during the heating phase (1−2 in Figure 2). Although by and large a linear relation existed between ln $p$ and $1/T$, at low concentration levels, under some conditions the behavior was somewhat peculiar as seen in Figure 6. The vapor pressure curve of R-507A is depicted for the sake of comparison. The flattened S shaped nature of the curve was pronounced when relatively high loading was used with pressures close to saturation pressure at $T_{ads}$. As a consequence, it has not been possible to correlate this property conclusively to date. It is possible that the adsorbed phase volume depends on pressure as well. In the cases where relative uptakes are less than 0.78, there exists a linear relation between ln $p$ and $1/T$. Data extracted from slopes yielding the isosteric heat of adsorption are presented in Figure 7. In general, the isosteric heat of adsorption in the case of R-507 shows a weak uptake dependence unlike in the case of methane.[23] The average value of isosteric heat of adsorption so obtained (21000 $J \cdot mol^{-1}$) is about 10 % less than that obtained from the Tóth and Langmuir correlations, where it enters as a correlating parameter.

A drawback of the desorption method of measurement is that if the isotherm has a point of inflection (as happens in IUPAC

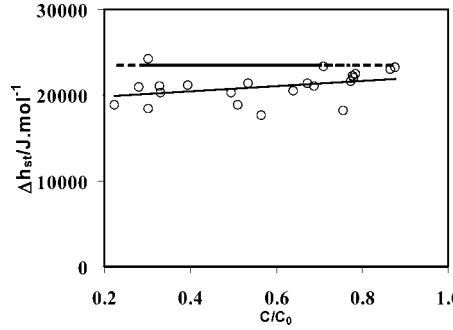


**Figure 7.** Uptake dependence of isosteric heat of adsorption. ○, Extracted from experimental data on pressure and temperature during isosteric heating; broken line, Langmuir and Tóth equation $\Delta h_{st}$ values; full line, best fit to experimentally extracted data.

type II isotherms at high uptakes) the method described for difference in concentrations will not hold well. Adsorption of HFC 134a on a Maxsorb II specimen at low temperatures and high pressures is known to tend toward a type II isotherm.[14] One of the presumptions is that the isotherm equations considered here can describe the adsorption phenomena which happens only in IUPAC type I isotherms for which the isotherm equations opted to hold well.

## Conclusions

Adsorption data for R-507A on a Maxsorb III specimen of activated carbon were obtained through desorption measurements. The measurements cover the temperature range of (5 to 70) °C and pressures up to 15 bar. The data were correlated to three popular isotherm equations. Low uptake isosteric heat of adsorption data were extracted from the experimental measurements, which appear to be well interpreted from that derived from the Tóth and Langmuir equations. The Tóth equation yields only a marginal improvement over the Langmuir equation. Adsorption of R-507A on a Maxsorb III specimen is somewhat less than that of HFC 134a on Maxsorb II indicating weaker Van der Waals forces in the former.

## Literature Cited

(1) Gray, I.; Luscombe, P.; McLean, L.; Sarathy, C. S. P.; Sheahen, P.; Srinivasan, K. Improvement of air distribution in refrigerated vertical open front remote supermarket display cases *Int. J. Refrigeration* **2007**, *31*, 902–910.
(2) Palm, B. Refrigeration systems with minimum charge of refrigerant. *Appl. Thermal Eng.* **2007**, *27*, 1693–1701.
(3) Tsai, W. T. A review of environmental hazards and adsorption recovery of cleaning solvent hydrofluorocarbons (HCFCs). *J. Loss Prev. Process Ind.* **2002**, *15*, 147–157.
(4) Mahle, J J.; Buettner, L. C. Measurement and correlation of adsorption equilibria of refrigerant vapors on activated carbon. *Ind. Eng. Chem. Res.* **1994**, *33*, 346–354.
(5) Riedel, V.; Radekar, K. H.; Schroeder, H.; Wutzler, R. On thermodynamics of adsorption of some refrigerants, fluorohydrocarbons and hydrocarbons onto several commercial adsorbents. *Chem. Tech. (Leipzig)* **2000**, *52*, 19–23.
(6) Berlier, K.; Frere, M.; Bougard, J. Adsorption of dichlorodifluoromethane, chlorodifluoromethane and chloropentafluoroethane on activated carbon. *J. Chem. Eng. Data* **1995**, *40*, 1137–1139.
(7) Ahn, N. G.; Kang, S. W.; Min, B. H.; Suh, S.S. Adsorption isotherms of tetrafluoromethane and hexafluoroethane on various adsorbents. *J. Chem. Eng. Data* **2006**, *51*, 451–456.
(8) Cho, S. Y.; Lee, Y. Y. Equilibria of 1,1,2-trichloro-1,2,2-trifluoroethane on activated carbons. *Ind. Eng. Chem. Res.* **1995**, *34*, 2468–2472.
(9) Park, H. M.; Moon, D. J. Adsorption equilibria of CFC-115 on activated charcoal. *J. Chem. Eng. Data* **2003**, *48*, 908–910.
(10) Moon, D. J.; Chung, M. J.; Cho, S. Y.; Ahn, B. S.; Park, H. M. Adsorption equilibria of chloropentafluoroethane and pentafluoroethane on activated carbon pellet. *J. Chem. Eng. Data* **1998**, *43*, 861–864.

(11) Siddye, M. A.; Wang, Q.; Chen, G. Evaluation of adsorption equilibrium and thermodynamic performance of R-123 (2,2-dichloro-1,1,1-trifluoroethane) - activated carbon working pair. *Energy Fuels* **2007**, *21*, 1169–1172.

(12) Croft, D. T. Adsorbent evaluation and adsorption equilibrium data for R-123, R-134a, and toluene on selected activated carbons, silica gels, and polymeric resins. Report No. ERDEC-CR-227, Edgewood Research Development and Engineering Center: Aberdeen Proving Ground MD, 1997.

(13) Tanada, S; Kawasaki, N.; Nakamura, T.; Ohue, T.; Abe, I. Adsorbability of 1,1,1,2-tetrafluoroethane (HFC134a) onto Plasma-treated activated carbon in $CF_4$ and $CCl_4$. *J. Colloid Interface Sci.* **1997**, *191*, 337–340.

(14) Akkimaradi, B. S.; Prasad, M.; Dutta, P.; Srinivasan, K. Adsorption of 1,1,1,2-tetrafluoroethane on activated charcoal. *J. Chem. Eng. Data* **2001**, *46*, 417–422.

(15) Tan, Z.; Xu, Y.; Wang, R.; Wu, J.; Deng, Y. Study on the adsorption characteristics of activated carbon-R134a. *Acta Energ. Sol. Sin.* **2000**, *21*, 128–132.

(16) Lin, S. H.; Lin, R. C. Adsorption of 1,1,1,2-tetrafluoroethane on various adsorbents. *J. Environ. Eng.* **1999**, *125*, 1048–1053.

(17) Tsai, W. T.; Chang, C. Y.; Ho, C. Y.; Chen, L. Y. Adsorption properties and breakthrough model of 1,1-dichloro-1-fluoroethane on granular activated carbon and activated carbon fiber. *Sep. Sci. Technol.* **2000**, *35*, 1635–1650.

(18) Akkimaradi, B. S.; Prasad, M.; Dutta, P.; Srinivasan, K. Effect of packing density and adsorption parameters on throughput of an adsorption compressor. *Carbon* **2002**, *40*, 2855–2859.

(19) Banker, N. D.; Prasad, M.; Srinivasan, K. Performance analysis of activated carbon + HFC 134a adsorption coolers. *Carbon* **2004**, *42*, 113–123.

(20) Banker, N. D. Development of an activated carbon + HFC 134a adsorption refrigeration system. PhD Thesis, Indian Institute of Science, Bangalore, 2006.

(21) Saha, B. B.; Chakraborty, A.; Koyama, S.; Srinivasan, K.; Ng, K. C.; Kashiwagi, T.; Dutta, P. Thermodynamic formalism of minimum heat source temperature for driving advanced adsorption cooling device. *Appl. Phys. Lett.* **2007**, *91*, 111902.

(22) Prakash, M.; Mattern, A.; Prasad, M.; Sant, R.; Subramanya; Srinivasan, K. Adsorption parameters of activated charcoal from desorption studies. *Carbon* **2000**, *38*, 1163–1168.

(23) Saha, B. B.; Koyama, S.; El Sharkawy, I. I.; Habib, K; Srinivasan, K.; Dutta, P. Evaluation of adsorption parameters and heat of adsorption through desorption measurements. *J. Chem. Eng. Data* **2007**, *52*, 2419–2424.

(24) REFPROP. Reference Fluid Thermodynamic and Transport Properties. NIST Standard Reference Data Bases 23, Version 7.0, 2002.

(25) Solkane 507 Thermodynamics, Product BulletinNoT/09.04/05/E. Solvay Fluor, Hannover.

Received for review March 25, 2008. Accepted June 8, 2008. This work was partially supported by the Ministry of Education, Science, Sports and Culture (MEXT), Japan, "Science and Technology Project", Project No. 18650205.

JE800204P